Local-field effect on the spontaneous radiative emission rate

Chang-Kui Duan,* Hongli Wen, and Peter A. Tanner†

Department of Biology and Chemistry, City University of Hong Kong, Tat Chee Avenue, Kowloon, Hong Kong S.A.R., People's Republic of China

(Received 21 April 2011; revised manuscript received 18 May 2011; published 24 June 2011)

The effect of the dielectric medium upon the spontaneous emission rate was investigated using lead borate glass of various compositions lightly doped with the Eu^{3+} lanthanide ion. A dual approach used the variation of (i) electric dipole/magnetic dipole (ED/MD) emission rates from spectral integrations and (ii) absolute ED emission rates from lifetime measurements for comparison with the variation of the refractive index of the glass medium. Contrary to a previous study [Phys. Rev. Lett. **91**, 203903 (2003)], the results show the relevance of the virtual-cavity model in this case. The MD emission rates were taken to follow the n^3 increase in density of photon states in the medium. The justifications for employing Eu^{3+} for identifying the appropriate model are given.

DOI: 10.1103/PhysRevB.83.245123 PACS number(s): 42.65.Pc, 33.20.Kf, 33.90.+h, 42.70.Ce

I. INTRODUCTION

Spontaneous emission of radiation is a fundamental property of matter. It is not only of great theoretical interest but also of practical importance in optical materials.[1] Although the spontaneous emission rate of an isolated emitter in vacuum is given in quantum mechanics textbooks in terms of interaction of the free electromagnetic field with the ionic or molecular emitter, the case of emitting ions, molecules, or nanoparticles surrounded by other polarizable atoms (including both ions and molecules) is subtler and has been subject to extensive theoretical[2–9] and experimental[2,10–16] investigations during the last few decades.

The enhancement (χ) of spontaneous emission rates for electric dipole (ED) transitions because of surrounding polarizable atoms is usually termed the *local-field* effect.[11] The most accepted models for this effect are originally based on macroscopic theory[2,3,17] and have been rederived more recently from a more fundamental microscopic theory, taking the interaction of the quantized electromagnetic field with the emitter and a uniformly distributed bath of atoms constituting the dielectric medium to the first order[7] and also confirmed under certain conditions to the second order in $n-1$.[8]

The two well-known macroscopic models are the virtual-cavity (VC) model and the real-cavity (RC) model. De Vries and Lagendijk[5] pointed out that if the emitters can be considered as "interstitial" impurities, the VC model (i.e., the Lorentz model) is applicable, whereas if the emitters can be considered as "substitutional" impurities, the RC model is relevant. Although many measurements on the emission lifetimes of optical materials are available in the literature, only a few specific experiments have been designed for the purpose of the discrimination between the two cavity models. Relevant experimental results have been critically re-examined in the context of the original criterion for the applicability of the two models.[17] However, it is still puzzling that although both Ce^{3+} and Eu^{3+} lanthanide ions are small cations of low polarizability, whose doping in solid-state hosts should have minimum impact on the surrounding media, the analysis of the allowed ED $5d$-$4f$ transition of Ce^{3+} ions in various crystals supports the VC model,[18] whereas the allowed induced ED $4f$-$4f$ transition of Eu^{3+} ions in glasses has been claimed to support the RC model.[14] The present study resolves this apparent conflict.

II. EXPERIMENT

The glass samples of composition $(99.6-z)(PbO).z(B_2O_3).0.4(0.5Eu_2O_3)$, where z was varied in the range of 20–70, were prepared by using Eu_2O_3 (99.99%, International Laboratory USA), PbO (99.9+%, Sigma-Aldrich), and H_3BO_3 (99.5%, Sigma-Aldrich) as starting materials. The components were milled, mixed together well, and melted at 1000 °C for 1 h. Then they were quenched and annealed below the glass transition temperature to eliminate internal mechanical stress. Samples were polished for room temperature refractive index measurements at wavelengths of 632.8 and 473 nm using a Metricon 2010/M prism coupler. These measurements at two wavelengths enabled the well-known empirical Cauchy formula $n(\lambda) = A + B/\lambda^2$ to be employed to derive the refractive index, n, at 612 nm for each sample. This wavelength corresponds to that of the $^5D_0 \rightarrow {}^7F_2$ emission band of Eu^{3+}. It was found that the refractive index values at 695 nm ($^5D_0 \rightarrow {}^7F_4$) are smaller by $\leqslant 0.8\%$ and those at 590 nm ($^5D_0 \rightarrow {}^7F_1$) are larger by $\leqslant 0.3\%$ than the corresponding values at 612 nm. Thus, in the calculations herein, a fixed value of the refractive index has been employed for all three wavelengths.

Room temperature excitation, emission spectra, and emission lifetimes were recorded by a Horiba Jobin Yvon Fluorolog spectrophotometer using a xenon lamp as the light source, and the signal was detected by a Hamamatsu R636 photomultiplier. The excitation and emission slits were 2 nm and 5 nm, respectively. The emission spectra were corrected for instrumental response by calibration with a standard lamp from the US National Institute of Standards and Technology.

III. RESULTS AND DISCUSSION

The enhancement (χ) factors for an ED transition because of the surrounding media (of the refractive index n) for the VC and RC models are as follows:[17]

$$[\Gamma(n)/\Gamma(1)]_{\text{virtual}} = \chi_{\text{virtual}} = n\left[\frac{2+n^2}{3}\right]^2 \qquad (1)$$

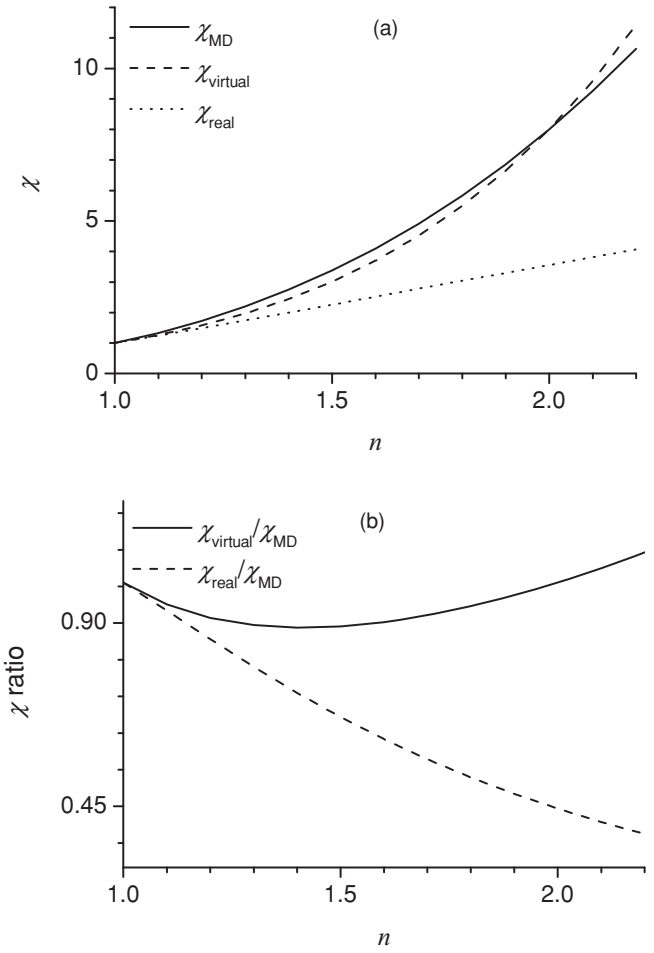

FIG. 1. The enhancement (χ) factors for emission rates because of the refractive index of the dielectric media (a) and their ratios (b).

$$[\Gamma(n)/\Gamma(1)]_{\text{real}} = \chi_{\text{real}} = n\left[\frac{3n^2}{2n^2+1}\right]^2 \tag{2}$$

Here, $\Gamma(n)$ and $\Gamma(1)$ are the spontaneous emission rates of the emitter embedded in a dielectric medium and in vacuum, respectively. The dependence of the spontaneous emission rate for a magnetic dipole (MD)-allowed transition is purely because of the n^3 increase in density of photon states,[10] i.e.,

$$[\Gamma(n)/\Gamma(1)]_{\text{mag}} = \chi_{\text{MD}} = n^3. \tag{3}$$

Figure 1(a) contrasts the dependence of the spontaneous emission intensity enhancement for ED transitions, according to the RC and VC models. The difference is larger above $n \sim 1.5$, and the VC model shows a dependence upon n similar to that for MD transitions. This point is emphasized in Fig. 1(b), where enhancement ratios are plotted, and it is referred to again later.

There are complications in experimental studies of the local-field effect when using rare earth ions, because the ED, MD, or even nonradiative contributions to the decay rate of the luminescent excited state may not have been clearly identified or separated. Furthermore, the ED line strengths for the forced dipole transitions may be sensitive to the arrangement of the surrounding atoms of the rare earth ion. An underlying assumption in the models for the local-field effect is that the ED line strength is independent of the environment of the emitting ion.

TABLE I. The measured emission rate ratios and derived spontaneous emission rates. $A(^7F_1)[\text{calc}] = 0.01465n^3$; $A(^7F_k)[\text{calc}] = [A(^7F_k)/A(^7F_1)] \times A(^7F_1)[\text{calc}]$; and $A_{\text{ED}} = 1/\tau_{\text{expt}} - A(^7F_1)[\text{calc}]$ are used to calculate the relevant rates.

Composition (z)	20	30	40	60	70
n	2.058	1.952	1.865	1.742	1.682
$A(^7F_2/)A(^7F_1)$	4.11	3.94	3.90	4.03	3.84
$A(^7F_4/)A(^7F_1)$	1.39	1.34	1.31	1.28	1.26
$A(^7F_4/)A(^7F_2)$	0.337	0.340	0.334	0.317	0.328
τ_{expt} (ms)	0.96	1.19	1.37	1.65	1.90
$A(^7F_1)[\text{calc}]$ $(\text{ms})^{-1}$	0.128	0.109	0.095	0.077	0.070
$A(^7F_2)[\text{calc}]$ $(\text{ms})^{-1}$	0.525	0.429	0.371	0.312	0.268
$A(^7F_4)[\text{calc}]$ $(\text{ms})^{-1}$	0.177	0.146	0.124	0.099	0.088
A_{ED} $(\text{ms})^{-1}$	0.92	0.73	0.63	0.53	0.46

Our strategy for the investigation of local-field effects, and distinction of the relevant valid model, has been to investigate the forced dipole luminescence of europium (Eu^{3+}) doped into lead borate glasses. Variation of the glass refractive index over a wide range is readily accomplished by variation of the glass composition. As mentioned earlier, it is therefore imperative to demonstrate that the ED strength remains constant during this variation.

The variation of the refractive index as a function of glass composition is displayed in Table I, and the range of values is from 1.682 for the boron-rich glass ($z = 70$) to 2.058 for the lead-rich glass ($z = 20$).

The room temperature excitation spectra of all samples recorded by monitoring the emission at 612 nm are plotted in Fig. 2. In the range of 450–550 nm, the spectra for all samples are of the same pattern and show the Eu^{3+} $^7F_{0,1} \rightarrow {}^5D_{1,2}$ absorption bands. The relative decrease of emission intensity for samples containing greater Pb contents for excitation in the $^5L_6$ region (peaking near 394 nm) shows the sharp decrease of penetration depth for the near-ultraviolet light into the samples with small z values due to absorption of Pb^{2+} ions.[19]

Figure 3 plots the normalized emission spectra for samples in the range of 570–730 nm under 464-nm excitation. The spectra are corrected to give the relative photon emission rate (photon flux, which is proportional to the number of photons detected, rather than luminescence intensity, which is proportional to the number of photons multiplied by photon energy). Interestingly, the emission spectra change only slightly with glass composition.

The induced ED transition is allowed for $^5D_0 \rightarrow {}^7F_{2,4}$ but forbidden for $^5D_0 \rightarrow {}^7F_{0,1,3}$, according to the well-known Judd selection rules.[20] The $^5D_0 \rightarrow {}^7F_1$ transition is allowed under MD selection rules, whereas the ED phonon-assisted $^5D_0 \rightarrow {}^7F_1$ transition obeys the same Judd selection rules and is forbidden.[20] The $^5D_0 \rightarrow {}^7F_{0,1,3}$ transitions may obtain very weak intensity because of mixing of $^7F_2$ (and, to a much smaller extent, $^7F_4$ and $^7F_6$) bases into the $^7F_{0,1,3}$ wavefunctions, which is termed J-mixing and has been treated theoretically.[21] The mixing of $^7F_2$ components into $^7F_1$ states is estimated to be on the order of magnitude of 1%, is

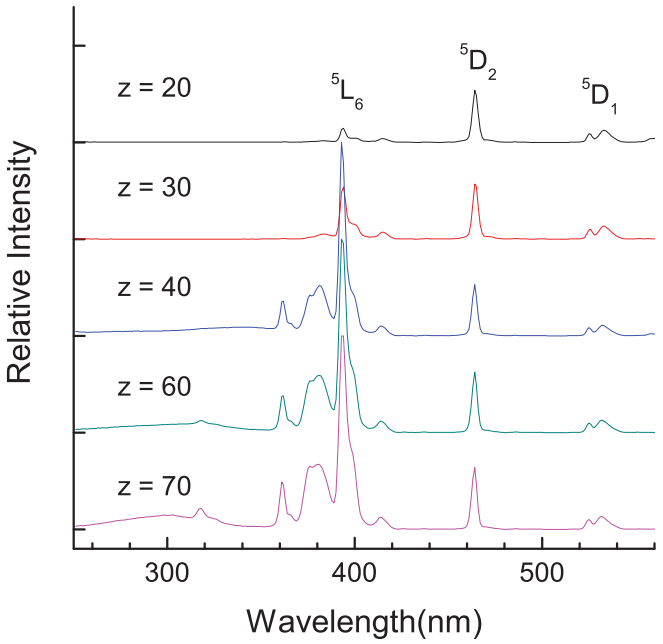

FIG. 2. (Color online) The excitation spectra of the glass samples doped with Eu^{3+} obtained by monitoring the 612-nm emission bands. The initial states are $^7F_{0,1}$, and some terminal states are marked.

independent of the refractive index, and has been neglected in the following analysis. Hence, in Fig. 3, the $^5D_0 \rightarrow {}^7F_{2,4}$ transitions are observed to be strong, whereas the $^5D_0 \rightarrow {}^7F_{0,3}$ transitions are very weak. By integration of the individual $^5D_0 \rightarrow {}^7F_{1,2,4}$ transition portions of the emission spectra, the ratios for the transition rates $A(^7F_2)/A(^7F_1)$ and $A(^7F_4)/A(^7F_1)$ can be derived (Table I). Because there is no local-field effect for nonmagnetic material and the MD line strength for the $^5D_0 \rightarrow {}^7F_1$ transition is relatively insensitive to the host material, the $^5D_0 \rightarrow {}^7F_1$ transition rate (in reciprocal milliseconds) can be well predicted in the absence of J-mixing:[1]

$$A(^7F_1)[\text{calc}] = 0.01465n^3. \quad (4)$$

Then from the ratios for the transition rates derived earlier and the values from Eq. (4) for $A(^7F_1)$[calc], the ED transition rates $A(^7F_k)$ ($k = 2,4$) were derived. The results are also listed in Table I.

The luminescence decay curves of $^5D_0$ were measured by detecting 612 nm with a spectral bandpass of 5 nm for glass samples of different compositions under different excitation wavelengths. All decay curves can be fitted reasonably well by monoexponential decay curves. The lifetimes change slightly when employing narrowband excitation wavelengths and detection emission wavelengths because of site selection. The broadband excitation and detection wavelengths were used to measure the average decay rates of most sites. The measured decay curves are shown in Fig. 4 and can be fitted with monoexponential decay functions quite well. The resultant lifetime (τ_{expt}) data are given in Table I. The change of τ_{expt} with the refractive index (or composition of the glass) is clearly more dramatic than reported in Kumar *et al.*,[14] where the variation of τ_{expt} with the refractive index was employed to demonstrate the conclusion that the local-field effect on the ED spontaneous emission rate follows the RC model. The 435-nm excitation employed in that study does not directly populate Eu^{3+} energy levels and gives an underlying, broad background emission on the Eu^{3+} bands.

The concentration of Eu^{3+} in our lead borate glass samples is reasonably low, and the gap between the luminescent $^5D_0$

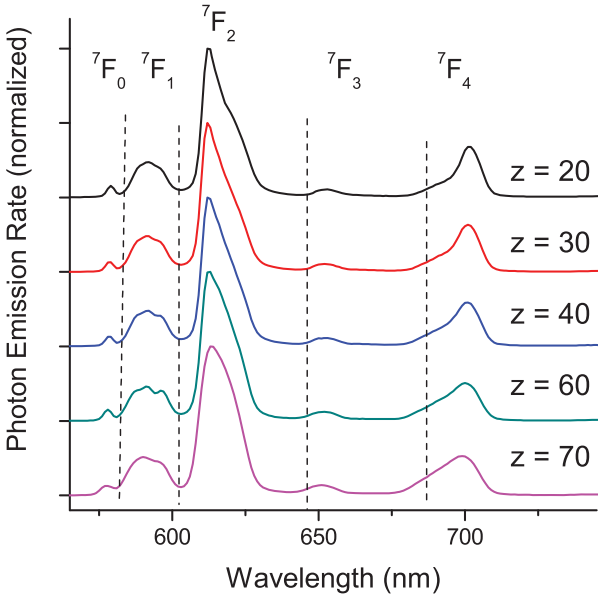

FIG. 3. (Color online) Luminescence spectra of the glass samples under 464-nm broadband excitation. The luminescent state is $^5D_0$, and terminal multiplets are marked. The relative emission rate for each $^5D_0 \rightarrow {}^7F_J$ ($J = 0$–4) transition can then be calculated by integration of these spectra, and the ratios $A(^7F_{2,4})/A(^7F_1)$ and $A(^7F_4)/A(^7F_2)$ can be derived.

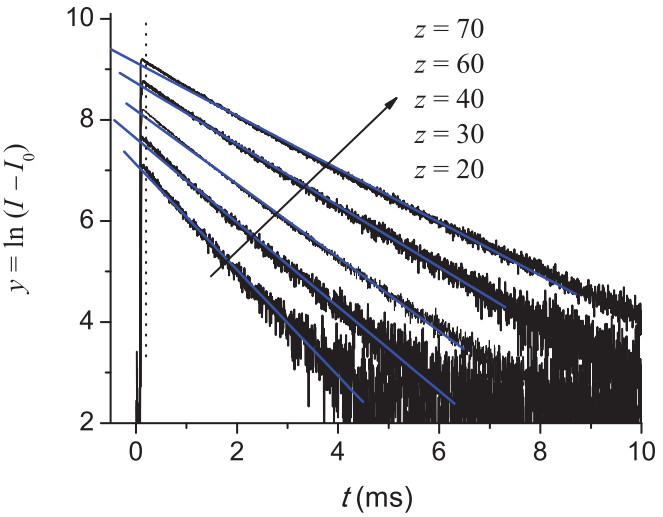

FIG. 4. (Color online) Emission decay curves for lead borate glasses of various compositions, doped with Eu^{3+}. The intensity I is measured for the 612-nm emission band under 464-nm broadband excitation, whereas I_0 is the signal determined in the $t = 0$ region when the sample is not excited; each of the straight lines is a linear fit of a curve in the range $(y_0, y_0 - 4)$, where y_0 is determined by the intercept of the curve with the vertical dotted line. The obtained lifetime data are listed in Table I and agree with those obtained under the excitation wavelength of 533 nm.

level and the next lower energy level, $^7F_6$, is $>10^4$ cm^{-1} and requires $\sim$10 phonons for the $^5D_0$–$^7F_6$ nonradiative decay via multiphonon relaxation. We therefore concur with Kumar *et al.*[14] that the decay of $^5D_0$ can be considered to be predominately a result of radiative decay. However, the radiative decay of $^5D_0$ is not purely by the ED mechanism; rather, it also includes a small but non-negligible contribution from the MD mechanism. Neglecting the rate because of nonradiative decay, and deducting the part of the decay rate because of the $^5D_0 \rightarrow {}^7F_1$ MD transition in Eq. (4), the $^5D_0$ total ED transition rate is obtained from

$$A_{\mathrm{ED}} = 1/\tau_{\mathrm{expt}} - A(^7F_1)[\mathrm{calc}]. \quad (5)$$

The results for A_{ED} are also listed in Table I, together with those for individual radiative channels.

The total, $^5D_0 \rightarrow {}^7F_2$, and $^5D_0 \rightarrow {}^7F_4$ ED rates are plotted against the enhancement factor for the RC model and the VC model in Fig. 5(a) and 5(b), respectively. To check the validity of the RC or VC model, the data have been fitted with $y =$ constant $\times\, x$ for each model (i.e., ED transition rate = constant $\times\, \chi$). None of the ED rates fall on the best fitted lines passing through the origin in Fig. 5(a) . This rules out the applicability

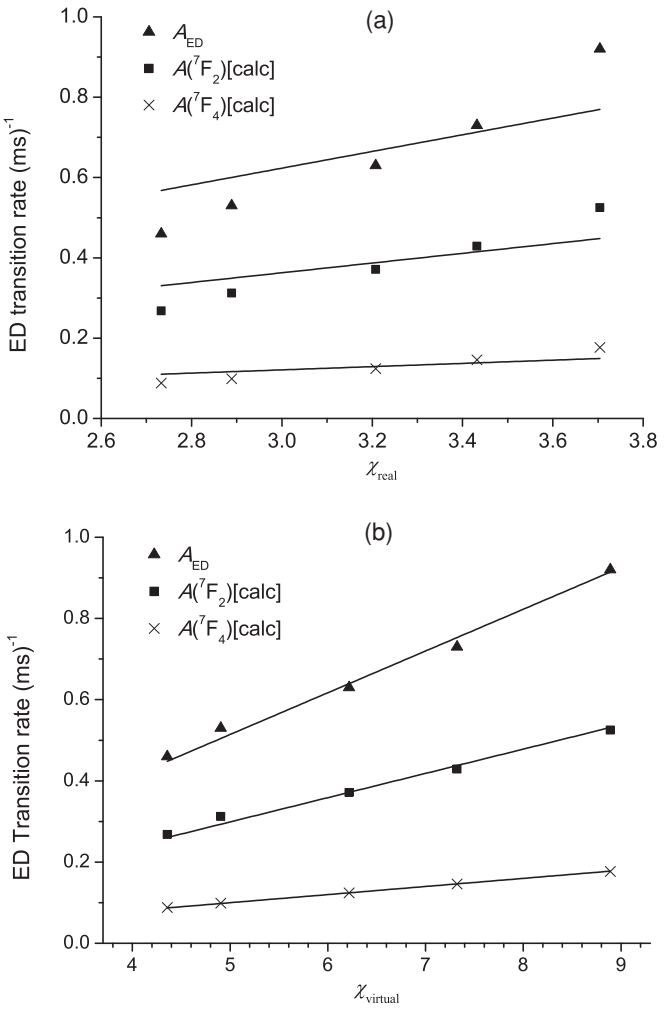

FIG. 5. Emission rates versus χ_{real} (a) and χ_{virtual} (b). The lines are the linear fittings of the data points for RC and VC models with $y =$ constant $\times\, x$.

of the RC model, contrary to the conclusion drawn in Kumar *et al.*[14] The fitting in Fig. 5(b) shows that all ED rates (i.e., the total, $^5D_0 \rightarrow {}^7F_2$, and $^5D_0 \rightarrow {}^7F_4$ rates) fall on the best fitted lines within the experimental error indicated roughly by the size of the data points.

In both the preceding analysis and the analyses of other studies, there is an underlying (and unjustified) assumption that the ED line strengths for the transitions involved do not vary with the modification of compositions of the dielectric media used for adjusting the refractive index. We now provide a justification for this assumption. According to Judd-Ofelt theory,[22,23] the ED line strengths for the $^5D_0 \rightarrow {}^7F_2$ and $^5D_0 \rightarrow {}^7F_4$ transitions are linearly related to the intensity parameters Ω_2 and Ω_4, respectively. These parameters have very different dependences upon the bond lengths (and bond angles) of neighboring ions. Hence, if the ED line strengths do vary appreciably with the glass compositions, then it cannot be expected that Ω_2 and Ω_4 vary in the same way; therefore, the ratio $A(^7F_4)/A(^7F_2)$ should depend on the composition and should differ for different samples. This ratio barely changes in Table I, and for all compositions $\Omega_2 = (6.03 \pm 0.19) \times 10^{-20}$ cm^2 and $\Omega_4 = (4.29 \pm 0.08) \times 10^{-20}$ cm^2, so the independence of ED line strengths upon the compositions can be fulfilled. This may be given the physical interpretation that although the composition of the glass changes, the statistical average of the distributions of the local arrangement of ligands for Eu^{3+} does not change dramatically.

It is evident from Fig. 1(b) that the ratio of VC-to-MD enhancement factors increases by only $\sim$10% when n changes from 1.682 to 2.058; at the same time, the ratio of the RC-to-MD enhancement factors decreases by >25%. The measured ED/MD ratios increase by $\sim$9.4%, 7%, and 10% for the total ED, $^5D_0 \rightarrow {}^7F_2$, and $^5D_0 \rightarrow {}^7F_4$ transitions, respectively. These increases are close to those expected for the VC model but are different from those for the RC model.

The systematic errors from the correction of emission spectra because of the response function of the photomultiplier tube used in recording the spectra may result in a scaling of all ratios for the $^7F_2/^7F_1$ or $^7F_4/^7F_1$ emission rates. The scaling factors (which may be different for $^7F_2$ and $^7F_4$) depend only on wavelength and do not change with composition, because the spectra show that the positions of the $^5D_0 \rightarrow {}^7F_2$ and $^5D_0 \rightarrow {}^7F_4$ bands do not change when the refractive index changes.

IV. CONCLUSION

The local-field effect of surrounding media to the emitting ions was studied experimentally using Eu^{3+} ions in lead borate glass of various compositions with a refractive index in the range of 1.682–2.058. Both the ratio for ED/MD emission rates derived from the integration of emission spectra and the absolute ED emission rates derived from decay lifetimes show that the enhancement of ED transition rates with a refractive index favors the VC model overwhelmingly over the RC model. This conclusion does not conflict with various other cases reported previously, which support the RC model, as justified in Duan *et al.*[17] The practical criterion initially set

out in de Vries and Lagendijk[5] can be reiterated here: when the emitter can be considered as an "interstitial" impurity in the sense that it is a cation of low polarizability (whose presence does not disturb the dielectric media), the VC model is applicable, whereas when the emitter dispels the dielectric media from the space occupied by the emitter and creates a real hole in the media, the RC model may be more relevant.

ACKNOWLEDGMENTS

We thank M. F. Reid (University of Canterbury, New Zealand) for helpful discussions. This work was supported by the Research Grants Council of Hong Kong (Project No. CityU 102609) and the National Natural Science Foundation of China (Projects No. 10874253 and No. 11074315).

*Present address: Department of Physics, University of Science and Technology of China, Hefei, Anhui 230026, People's Republic of China.

†bhtan@cityu.edu.hk

[1]M. H. V. Werts, R. T. F. Jukes, and J. W. Verhoeven, Phys. Chem. Chem. Phys. **4**, 1542 (2002).

[2]E. Yablonovitch, T. J. Gmitter, and R. Bhat, Phys. Rev. Lett. **61**, 2546 (1988).

[3]R. J. Glauber and M. Lewenstein, Phys. Rev. A **43**, 467 (1991).

[4]S. M. Barnett, B. Huttner, and R. Loudon, Phys. Rev. Lett. **68**, 3698 (1992).

[5]P. de Vries and A. Lagendijk, Phys. Rev. Lett. **81**, 1381 (1998).

[6]M. E. Crenshaw and C. M. Bowden, Phys. Rev. Lett. **85**, 1851 (2000).

[7]P. R. Berman and P. W. Milonni, Phys. Rev. Lett. **92**, 053601 (2004).

[8]H. Fu and P. R. Berman, Phys. Rev. A **72**, 022104 (2005).

[9]M. E. Crenshaw, Phys. Rev. A **78**, 053827 (2008).

[10]G. L. J. A. Rikken and Y. A. R. R. Kessener, Phys. Rev. Lett. **74**, 880 (1995).

[11]F. J. P. Schuurmans, D. T. N. de Lang, G. H. Wegdam, R. Sprik, and A. Lagendijk, Phys. Rev. Lett. **80**, 5077 (1998).

[12]R. S. Meltzer, S. P. Feofilov, B. Tissue, and H. B. Yuan, Phys. Rev. B **60**, R14012 (1999).

[13]H. Schniepp and V. Sandoghdar, Phys. Rev. Lett. **89**, 257403 (2002).

[14]G. M. Kumar, D. N. Rao, and G. S. Agarwal, Phys. Rev. Lett. **91**, 203903 (2003).

[15]S. F. Wuister, C. de M. Donegá, and A. Meijerink, J. Chem. Phys. **121**, 4310 (2004).

[16]L. Zampedri, M. Mattarelli, M. Montagna, and R. R. Gonçalves, Phys. Rev. B **75**, 073105 (2007).

[17]C.-K. Duan, M. F. Reid, and Z. Wang, Phys. Lett. A **343**, 474 (2005).

[18]C.-K. Duan and M. F. Reid, Curr. Appl. Phys. **6**, 348 (2006).

[19]H. L. Wen, G. H. Jia, C.-K. Duan, and P. A. Tanner, Phys. Chem. Chem. Phys. **12**, 9933 (2010).

[20]P. A. Tanner and C.-K. Duan, Coord. Chem. Rev. **254**, 3026 (2010).

[21]S. D. Xia and Y. M. Chen, J. Lumin. **33**, 228 (1985)

[22]B. R. Judd, Phys. Rev. **127**, 750 (1962).

[23]G. S. Ofelt, J. Chem. Phys. **37**, 511 (1962).